

# Calculation of bridging oxygen $^{17}\text{O}$ quadrupolar coupling parameters in alkali silicates: A combined ab initio investigation

Ted M. Clark, Philip J. Grandinetti\*

*Department of Chemistry, The Ohio State University, 120 W. 18th Avenue, Columbus, OH 43210-1173, USA*

Received 14 September 2004; received in revised form 20 January 2005

## Abstract

Ab initio band-structure calculations based on the density functional theory have been performed for several crystalline Li, Na, and K-silicates to obtain electric-field gradients (efg) for oxygen atoms. The efg for bridging oxygen environments in these compounds were also investigated by performing ab initio self-consistent field Hartree–Fock molecular orbital calculations on silicate clusters, and there is good agreement between these two approaches. By performing additional ab initio quantum chemistry calculations on model silicate clusters the factors influencing the  $^{17}\text{O}$  quadrupole coupling parameters for bridging oxygen environments in alkali silicates have been examined. The quadrupolar asymmetry parameter was found to be dependent on the Si–O–Si angle and the nature of the modifier cation, in agreement with previous studies. In contrast, the quadrupolar coupling constant was found to have a strong dependence on Si–O distance, as well as Si–O–Si angle and the nature of the modifier cation. Analytical expressions describing these dependencies are proposed, which should assist in describing the local environments of bridging oxygen in crystalline and amorphous materials.

© 2005 Elsevier Inc. All rights reserved.

*Keywords:* Oxygen-17; Silicates; Quadrupolar nuclei

## 1. Introduction

With the continued improvement of computational resources it has become increasingly common to use ab initio quantum methods for predicting the electronic structure in crystalline materials [1–13]. These methods are also extremely useful for interpreting experimental results, such as the NMR spectra of solids, particularly for materials or nuclei where it is difficult to obtain experimental results and establish clear relationships between structural parameters and measurable NMR parameters. Oxygen-17 is one such nuclei which, despite its potential for helping to elucidate the structure of both crystalline and disordered materials, has been hampered by a low natural abundance and large quadrupole interactions which make otherwise

routine solid-state NMR experiments, such as MAS, challenging.

Recently, we have reported relationships for obtaining the Si–O–Si bond angle and Si–O distance from the  $^{17}\text{O}$  quadrupolar coupling parameters of a bridging oxygen atom, i.e., the quadrupolar coupling constant,  $C_q$ , and the quadrupolar asymmetry parameter,  $\eta_q$ . These relationships were revealed through systematic ab initio calculations on model clusters and calibrated with experimental  $^{17}\text{O}$  data for extended networks [14]. We have recently used these relationships to interpret the two-dimensional DAS spectrum of silica glass [15]. This approach resulted in the experimental determination of the two-dimensional correlated distributions in Si–O distance and Si–O–Si angle, as well as the determination of the distribution of Si–O–Si bond angles in this archetypical glass former.

To extend this approach to network-modified silicate glasses requires an understanding of how the

\*Corresponding author. Fax: +1 614 292 1685.

*E-mail address:* [grandinetti.1@osu.edu](mailto:grandinetti.1@osu.edu) (P.J. Grandinetti).

electric-field gradient (efg) for a bridging oxygen is affected by changes in structural parameters, including the presence of modifier cations. In an earlier investigation of alkali silicates, obtained using ab initio methods on model clusters representing typical bridging oxygen environments in lithium, sodium, and potassium silicates we began this task and demonstrated that several structural variables influence the bridging oxygen O-17 efg [16,17]. A more recent computational investigation of molecular dynamic simulated sodium silicate glasses supported many (but not all) of these general trends [13].

Thus, to investigate network-modified silicate glasses in a manner comparable to that performed for silica requires analytical expressions for bridging oxygen efg parameters that account for the relevant structural parameters. These parameters include the Si–O distances [13,18,19,14], Si–O–Si angles [20–22], and the field strength and number of network-modifier cations coordinated to the bridging oxygen atom [16,17]. Thus, suitable expression for the  $^{17}\text{O}$  quadrupolar coupling parameters are

$$C_q(\Omega, n_M) = a \left( \frac{1}{2} + \frac{\cos \Omega}{\cos \Omega - 1} \right)^\alpha + m_d(d_{\text{TO}} - d_{\text{TO}}^\circ) + n_M \Delta C_q^M, \quad (1)$$

$$\eta_q(\Omega, n_M) = b \left( \frac{1}{2} - \frac{\cos \Omega}{\cos \Omega - 1} \right)^\beta + \Delta \eta_q^M(n_M), \quad (2)$$

where  $\Omega$  is the Si–O–Si bond angle,  $d_{\text{TO}}$  is the average silicon–oxygen bond distance,  $m_d$  is a term (in MHz/Å) accounting for the distance dependence of  $C_q$ , with  $n_M \Delta C_q^M$  and  $\Delta \eta_q^M(n_M)$  accounting for contributions from  $n_M$  modifier cations coordinated to the bridging oxygen [14,17,15].

We will show here that the general trends described by these expressions are confirmed by ab initio calculations on model clusters. Additionally, in order to calibrate these expression, we will employ periodic density functional theory (DFT) calculations to determine the efg for bridging oxygen atoms in a variety of crystalline alkali silicates, since insufficient experimental  $^{17}\text{O}$  data exists to do so otherwise.

## 2. Methods

### 2.1. MO-cluster calculations

The electric-field gradients for bridging oxygen environments in these compounds were investigated by performing ab initio self-consistent field molecular orbital calculations on silicate clusters (MO-cluster calculations) using GAUSSIAN98 [23]. These calculations were performed at a restricted Hartree–Fock level with a  $6-31+G(d)$  basis set for all atoms.

Calculated efg tensor elements are related to the quadrupolar coupling constant,  $C_q$ , and quadrupolar coupling asymmetry parameter,  $\eta_q$ , according to

$$C_q = e^2 Q \langle q_{zz} \rangle / h \quad \text{and} \quad \eta_q = \frac{\langle q_{xx} \rangle - \langle q_{yy} \rangle}{\langle q_{zz} \rangle}, \quad (3)$$

where  $e\langle q_{xx} \rangle$ ,  $e\langle q_{yy} \rangle$ , and  $e\langle q_{zz} \rangle$  are the principal components of the electric-field gradient tensor defined such that  $|\langle q_{zz} \rangle| > |\langle q_{yy} \rangle| > |\langle q_{xx} \rangle|$  and  $Q$  is the nuclear electric quadrupole moment. For  $^{17}\text{O}$  a value of  $e^2 Q / h = -6.11$  MHz a.u.<sup>3</sup> was used to convert the  $q_{zz}$  output from Gaussian into the  $^{17}\text{O}$  quadrupolar coupling constant.

### 2.2. LAPW calculations

These calculations were based on the density functional theory (DFT) using the generalized gradient approximation (GGA) for the exchange and correlation potentials [24,25]. The full-potential, linearized, augmented plane-wave (LAPW) package WIEN97 [26] was used. In the LAPW method, the unit cell is divided into spheres centered at the atomic positions and an interstitial region. For the interstitial region, the basis set consists of plane waves which are augmented by atomic-like solutions inside the spheres. Sphere radii of 1.45, 1.50, 1.65, 1.45, 1.35 a.u. were used for Li, Na, K, Si, and O atoms, respectively. The cutoff for the plane wave basis set was chosen as  $R_{\text{mt}} K_{\text{max}} = 6.75$ , where  $R_{\text{mt}}$  corresponds to the smallest atomic sphere radii and  $K_{\text{max}}$  is the plane wave cutoff. These parameters typically resulted in more than 7000 LAPWs being used in our basis sets. Additional calculations confirmed that these results were well converged for these cutoff values. To treat the semicore states for silicon and oxygen additional local orbitals were employed. The number of  $k$  points in the irreducible Brillouin zone (IBZ) for the calculations ranged from 12 to 16. Nonspin-polarized calculations were studied in all cases. The LAPW calculations were computationally expensive, typically requiring more than a week to reach convergence when run on a SGI<sup>®</sup> Origin<sup>®</sup> 200 computer. These time constraints precluded the use of additional DFT supercell calculations for the investigation of possible crystalline distortions. The conversion factor for the full-crystal calculations of the quadrupolar coupling constant is given in Ref. [4].

## 3. Results and discussion

The  $^{17}\text{O}$  quadrupolar coupling parameters were calculated using the LAPW approach for several alkali silicates with reported crystal structures. The results are shown in Table 1. For two of the compounds, i.e.,  $\text{Li}_2\text{SiO}_3$  and  $\text{Li}_2\text{Si}_2\text{O}_5$ , several crystal structures have

Table 1  
 $^{17}\text{O}$  ab initio calculated results for the bridging oxygen sites in crystalline alkali silicates

Compound	Si–O–Si ( $^\circ$ )	SiO distances( $\text{\AA}$ )	Modifiers	Ref.	$C_q(\text{LAPW})(\text{MHz})$	$\eta_q(\text{LAPW})$	$C_q(\text{MO})(\text{MHz})$	$\eta_q(\text{MO})$	Ratio
$\text{Li}_2\text{SiO}_3$	124.6	1.68, 1.68	2 Li	[27]	−4.00	0.66	−4.09	0.58	0.98
$\text{Li}_2\text{SiO}_3$	133.0	1.55, 1.65	2 Li	[28]	−3.40	0.47	−3.77	0.32	0.90
$\text{Li}_2\text{SiO}_3$	126.5	1.64, 1.66	2 Li	[29]	−4.00	0.55	−4.17	0.48	0.96
$\text{Li}_2\text{SiO}_3$	124.1	1.68, 1.68	2 Li	[30]	−3.97	0.69	−4.12	0.61	0.96
$\text{Li}_2\text{Si}_2\text{O}_5$	158.6	1.61, 1.61	None	[31]	−5.25	0.09	−6.29	0.05	0.84
	129.4	1.64, 1.65	1 Li		−4.51	0.65	−4.84	0.74	0.93
$\text{Li}_2\text{Si}_2\text{O}_5$	156	1.61, 1.61	None	[32]	−5.18	0.10	−6.18	0.08	0.84
	132	1.58, 1.68	1 Li		−4.40	0.58	−4.89	0.69	0.90
$\text{Na}_2\text{SiO}_3$	133.7	1.67, 1.68	2 Na	[33]	−4.40 (−4.46)	0.54 (0.52)	−5.20	0.49	0.85
$\beta\text{-Na}_2\text{Si}_2\text{O}_5$	136.5	1.63, 1.63	1 Na	[34]	−4.55 (−4.68)	0.34 (0.12)	−5.44	0.36	0.84
	137	1.64, 1.64	1 Na		−4.63 (−4.77)	0.42 (0.41)	−5.59	0.44	0.83
	135	1.64, 1.64	1 Na		−4.57 (−4.67)	0.42 (0.42)	−5.51	0.55	0.83
	160	1.61, 1.61	None	[35]	−5.70 (−5.39)	0.09 (0.13)	−6.46	0.06	0.88
$\alpha\text{-Na}_2\text{Si}_2\text{O}_5$	138.9	1.64, 1.64	1 Na		−4.70 (−4.83)	0.40 (0.37)	−5.64	0.36	0.83
	123.4	1.63, 1.82 <sup>a</sup>	2 Na	[36]	−4.13	0.58	−4.19	0.68	0.98
$\text{Na}_2\text{Si}_3\text{O}_7$	158.4	1.59, 1.76 <sup>a</sup>	1 Na		−5.78	0.16	−6.37	0.26	0.90
	138	1.62, 1.78 <sup>a</sup>	1 Na		−4.81	0.36	−5.70	0.50	0.84
	132.8	1.66, 1.66	2 Na		−3.96	0.36	−4.93	0.50	0.80
	134.7	1.64, 1.66	2 K	[37]	−4.65	0.32	−5.56	0.41	0.84
$\text{K}_4\text{Si}_8\text{O}_{18}$	141.7	1.59, 1.78	2 K		−4.75	0.20	−5.00	0.22	0.95
	145.3	1.60, 1.65	None	[38]	−4.75	0.15	−6.16	0.13	0.77
	139.3	1.62, 1.64	1 K		−4.94	0.24	−5.60	0.19	0.88
	138.3	1.63, 1.64	1 K		−4.91	0.28	−5.52	0.28	0.89
	144.4	1.59, 1.66	1 K		−4.64	0.13	−5.93	0.27	0.78
	133.5	1.62, 1.64	1 K		−4.60	0.39	−5.64	0.43	0.82
	141.2	1.61, 1.64	None		−4.90	0.22	−5.99	0.21	0.82
	148.0	1.60, 1.61	None		−5.17	0.26	−6.02	0.19	0.86

Calculations were performed using the LAPW and MO-cluster methods. LAPW values in parentheses are calculated values from Ref. [13]. Ratio value in last column refers to  $C_q(\text{LAPW})/C_q(\text{MO})$ .

<sup>a</sup>Denotes an atypical bridging oxygen site bonded to tetrahedral and octahedral silicon atoms.

been proposed. Calculations were performed for each of these plausible crystal structure in order to obtain a maximum number of bridging oxygen environments with predicted  $C_q$  and  $\eta_q$  values. The bridging oxygen sites in these compounds are structurally diverse in terms of Si–O–Si angle, Si–O distances, and the type and number of modifiers present.

The LAPW predicted results agree with  $C_q$  and  $\eta_q$  values determined experimentally by MAS NMR spectroscopy. Experimental results for these compounds include  $C_q = 4.20(0.2)$  MHz,  $\eta_q = 0.58(0.05)$  for  $\text{Na}_2\text{SiO}_3$  [17],  $C_q = 5.74(0.2)$ ,  $4.67(0.2)$  MHz,  $\eta_q = 0.2(0.1)$ ,  $0.3(0.1)$ , for the two bridging oxygen sites in  $\alpha\text{-Na}_2\text{Si}_2\text{O}_5$  [39], and  $C_q = 4.45(0.05)$ ,  $4.90(0.05)$  MHz,  $\eta_q = 0.35(0.05)$ ,  $0.20(0.05)$ , for the two bridging oxygen sites in  $\text{K}_2\text{Si}_4\text{O}_9$  [40], respectively. This close agreement is expected, since the LAPW approach has accurately predicted the electronic structure in a wide variety of crystalline compounds, including other silicate minerals [1,4,11,41]. The results are also in good agreement with those previously investigated using periodic boundary conditions [13].

Molecular orbital (MO) cluster calculations were performed for these same crystalline sites, and the results are included in Table 1. Clusters were constructed based on the reported structural parameters, and included silicon atoms with accurate nearest-neighbor distances. Terminal oxygen atoms were capped with hydrogen atoms, resulting in clusters with the formulae  $(\text{OH})_3\text{Si-O-Si}(\text{OH})_3$ ,  $\text{M}[(\text{OH})_3\text{Si-O-Si}(\text{OH})_3]^+$ , and  $\text{M}_2[(\text{OH})_3\text{Si-O-Si}(\text{OH})_3]^{2+}$ , where M = Na, Li, or K, as shown in Fig. 1, an approach consistent with other investigations of bridging oxygen sites in silicates [16,17]. Bridging oxygen atoms bonded to tetrahedral and octahedral silicon atoms were examined in a similar manner, resulting in clusters with the formulae  $\text{M}[(\text{OH})_3\text{Si-O-Si}(\text{OH})_5]^-$  and  $\text{M}_2[(\text{OH})_3\text{Si-O-Si}(\text{OH})_5]$ .

The  $C_q$  values calculated by the LAPW approach are consistently smaller than those calculated by the MO-cluster approach. By introducing a scaling factor of 0.85 for the MO calculated results both sets of  $C_q$  values are brought into good agreement, shown in Fig. 2A. Such a scaling factor is commonly required for MO calculations

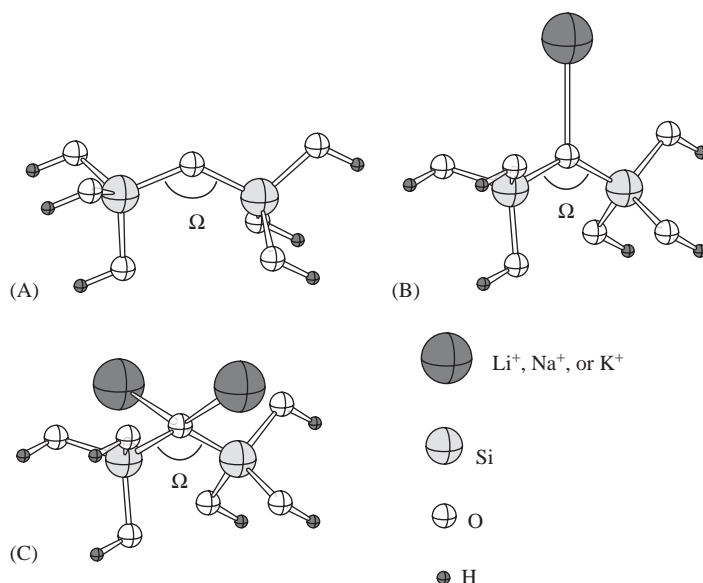


Fig. 1. Model clusters for bridging oxygen sites with (A) zero, (B) one, and (C) two modifier cations.

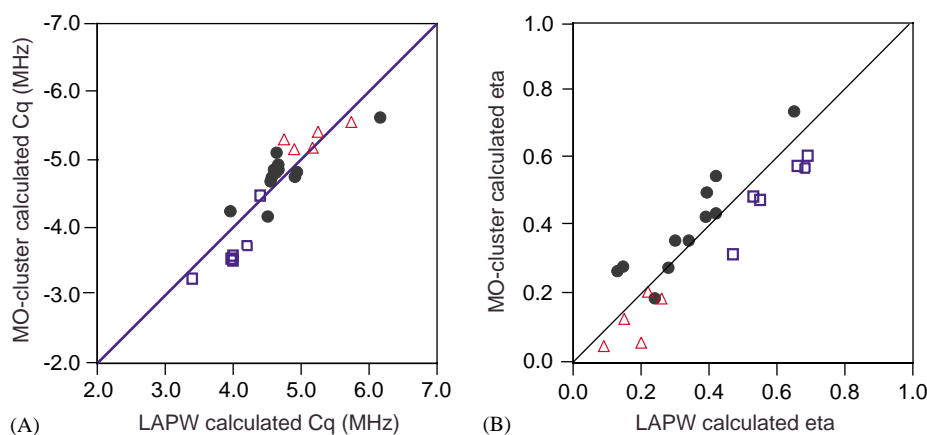


Fig. 2. Calculation of (A)  $C_q$  and (B)  $\eta_q$  for the crystalline alkali silicates listed in Table 1 by LAPW and MO-cluster methods. Symbols represent results for clusters with two modifiers (open squares), one modifier (filled circles), and no modifiers (open triangles).  $C_q$  values calculated by the MO-cluster method have been scaled by a factor of 0.85. The diagonal line depicts perfect agreement for each set of calculations.

of  $C_q$ , as discussed previously [17,16,42–44]. The agreement between calculated  $\eta_q$  values is poorer than that of the  $C_q$  values, and small systematic differences are evident for the  $\eta_q$  calculations, as shown in Fig. 2B. The MO calculated  $\eta_q$  values for clusters with one modifier are greater than those calculated by the LAPW method, and the MO calculated values for zero or two modifiers are smaller than those calculated by the LAPW method. These differences could be attributed to several factors, such as the lack of counter-ions for the alkali modifiers, or by neglecting the  $Q$ -species of the silicon atoms in the cluster. Clearly, however, it is possible to predict general trends between  $^{17}\text{O}$  quadrupolar coupling parameters for bridging oxygen atoms and local environment if the model clusters are in good agreement with the actual structure.

Having determined a suitable calibration for  $C_q$  values calculated by this MO approach, ab initio calculations were then performed for model clusters of bridging oxygen atoms coordinated with alkali cations. In these calculations the Si–O distances for the bridging oxygen were fixed (and symmetric) and the Si–O–Si angle varied. Either one or two alkali cations were coordinated to the bridging oxygen atoms and placed at distances typically found in crystalline compounds [16,17]. Representative trends in  $C_q$  and  $\eta_q$  values are shown in Fig. 3. The effect of Si–O distance on  $C_q$  is clear, with the magnitude of  $C_q$  increasing as the Si–O distance increases. This result is consistent with previous findings [13,14,18,19], and supports the inclusion of Si–O distance as a structural parameters affecting  $C_q$  in Eq. (1). In contrast, the quadrupolar asymmetry

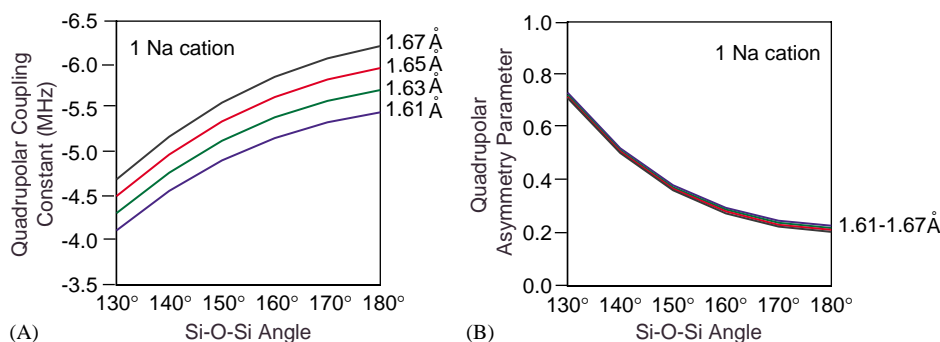


Fig. 3. Ab initio predicted trends in (A)  $C_q$  and (B)  $\eta_q$  as a function of Si–O–Si angle with Si–O distance held constant. Calculations were performed using a MO approach for a model cluster including one  $\text{Na}^+$  cation at a distance of  $2.5 \text{ \AA}$  from the bridging oxygen atom.

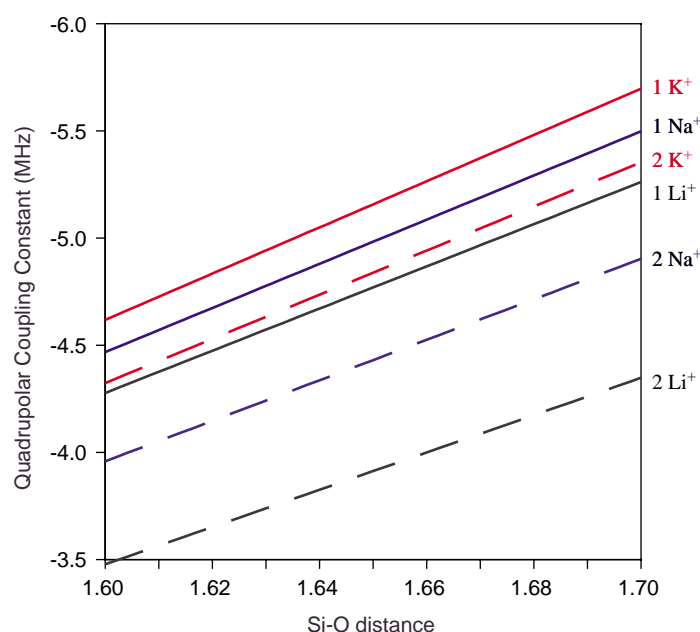


Fig. 4. Ab initio predicted trends in  $C_q$  (scaled by 0.85) with a fixed Si–O–Si angle of  $140^\circ$  and  $d(\text{Si–O})$  varied. Calculations were performed using a MO approach for a model cluster with cations at a fixed distance;  $\text{Li}^+$  at  $2.0 \text{ \AA}$ ,  $\text{Na}^+$  at  $2.5 \text{ \AA}$ , and  $\text{K}^+$  at  $2.8 \text{ \AA}$ . Solid lines are for clusters with one cation and dashed lines for clusters with two cations.

parameter is less sensitive to Si–O distance (Fig. 3B), a finding also consistent with previous results [12,14], and so a Si–O distances dependence is not appropriate for Eq. (2).

The influence of cation modifiers and Si–O distance for a fixed Si–O–Si angle are shown in Fig. 4. Here,  $C_q$  results are shown for a Si–O–Si angle of  $140^\circ$ , a bridging oxygen angle typically found in crystalline alkali silicates. The trends shown in Fig. 4 indicate that the nature and number of coordinating network modifiers clearly influence  $C_q$  for a given Si–O distance and Si–O–Si angle. As the number and field strength of the cation increases, the  $C_q$  values are systematically shifted to lower magnitudes. Also, the affect of Si–O distance on  $C_q$  does not appear to be strongly dependent on the

nature and number of coordinating cations, suggesting that the distance dependence for  $C_q$  in Eq. (2) will be similar for the alkali silicates considered here.

The  $C_q$  values were then calculated using the MO-approach for alkali-modified bridging oxygen sites with one or two modifier cations for a wide range of structures. For these model clusters the Si–O distances ranged  $1.6\text{--}1.7 \text{ \AA}$  and Si–O–Si angles ranged from  $125$  to  $180^\circ$ . These results have been fit using Eq. (2), and the parameters included in Table 2.

A somewhat different approach was used to describe  $\eta_q$  as a function of structural parameters. Instead of using  $\eta_q$  values calculated by a MO-approach to determine the parameters in Eq. (2), we have chosen to perform a least-squares fit of Eq. (2) to the LAPW

calculated results. The resulting fits are shown in Fig. 5 and best-fit parameters are given in Table 2. This approach was taken because the  $\eta_q$  values calculated by the MO-approach for these clusters displayed poorer agreement with the LAPW calculated values than did the  $C_q$  values. In comparison with previously reported trends based strictly on ab initio calculations for model

clusters [16,17], these results generally have smaller  $\Delta\eta^M$  values. This suggests that the large systematic shifts proposed earlier overstate the importance of coordinating cations on  $\eta_q$ . When the efg is calculated using a more complete description of the bridging oxygen environment (as in the LAPW calculations), the importance of the cations on  $\eta_q$  is mitigated with respect to what is suggested by model cluster calculations. If counter-ions were included in the model-cluster description of cation-modified bridging oxygen sites, it is likely that a similar result would also be obtained.

A comparison of the Si–O–Si angles and Si–O distances predicted by Eqs. (1) and (2) with the LAPW calculated results is shown in Fig. 6. The Si–O–Si angles in Fig. 6A are predicted from  $\eta_q$  with knowledge of the correct number modifier cations. As was the case for silica polymorphs,  $\eta_q$  appears to be a reliable probe of Si–O–Si angle. With the Si–O–Si angle determined by  $\eta_q$ , Eq. (1) is used to predict the Si–O distance from  $C_q$ , as shown in Fig. 6B. With the Si–O–Si and Si–O distance determined, it is also possible to determine the Si–Si distance, given in Fig. 6C. Here, we again assume that we know the number of cations near the bridging

Table 2  
Best-fit parameters for Eqs. (1) and (2)

Cation	$C_q$ dependence					$\eta_q$ dependence		
	$a$ (MHz)	$\alpha$	$\Delta C_q^M$ (MHz)	$d_{\text{T-O}}^M$ (Å)	$m_d$ (MHz/Å)	$b$	$\beta$	$\Delta\eta_q^M$
None	−6.53	1.80	0.00	1.654	−12.86	5.03	1.09	0.000
1 Li <sup>+</sup>	−5.90	1.80	0.68	1.61	−9.50	5.03	1.09	0.183
2 Li <sup>+</sup>	−5.90	1.80	0.72	1.61	−7.71	5.03	1.09	0.034
1 Na <sup>+</sup>	−5.90	1.80	0.57	1.61	−11.18	5.03	1.09	0.083
2 Na <sup>+</sup>	−5.90	1.80	0.57	1.61	−9.05	5.03	1.09	0.032
1 K <sup>+</sup>	−5.90	1.80	0.48	1.61	−10.66	5.03	1.09	0.000
2 K <sup>+</sup>	−5.90	1.80	0.50	1.61	−9.50	5.03	1.09	0.000

Parameters for the cluster without modifier cations are from Ref. [14].

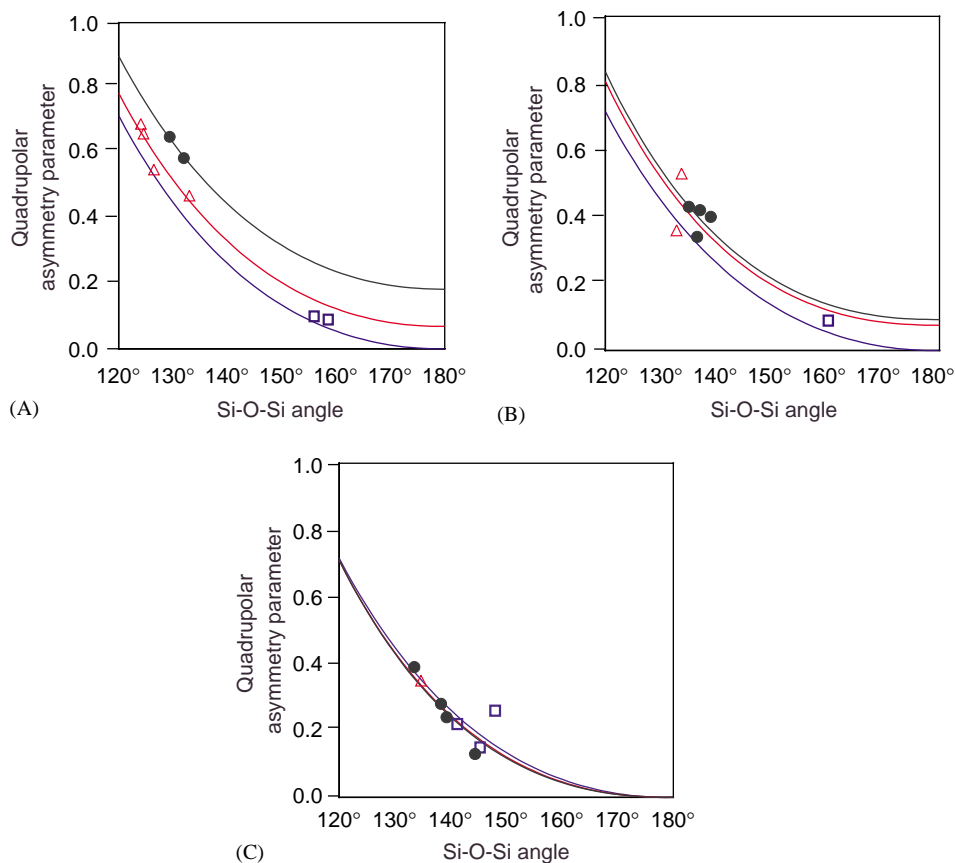


Fig. 5. Plots of quadrupolar asymmetry parameter versus Si–O–Si angle for (A) lithium silicates, (B) sodium silicates, and (C) potassium silicates. The LAPW calculated results are shown for sites with no modifiers (open squares), one modifier (filled circles), and two modifiers (open triangles). Solid lines were obtained from Eq. (2), for one, two, and zero modifiers, shown top to bottom, respectively. Best-fit parameters, using Eq. (2), are included in Table 2.



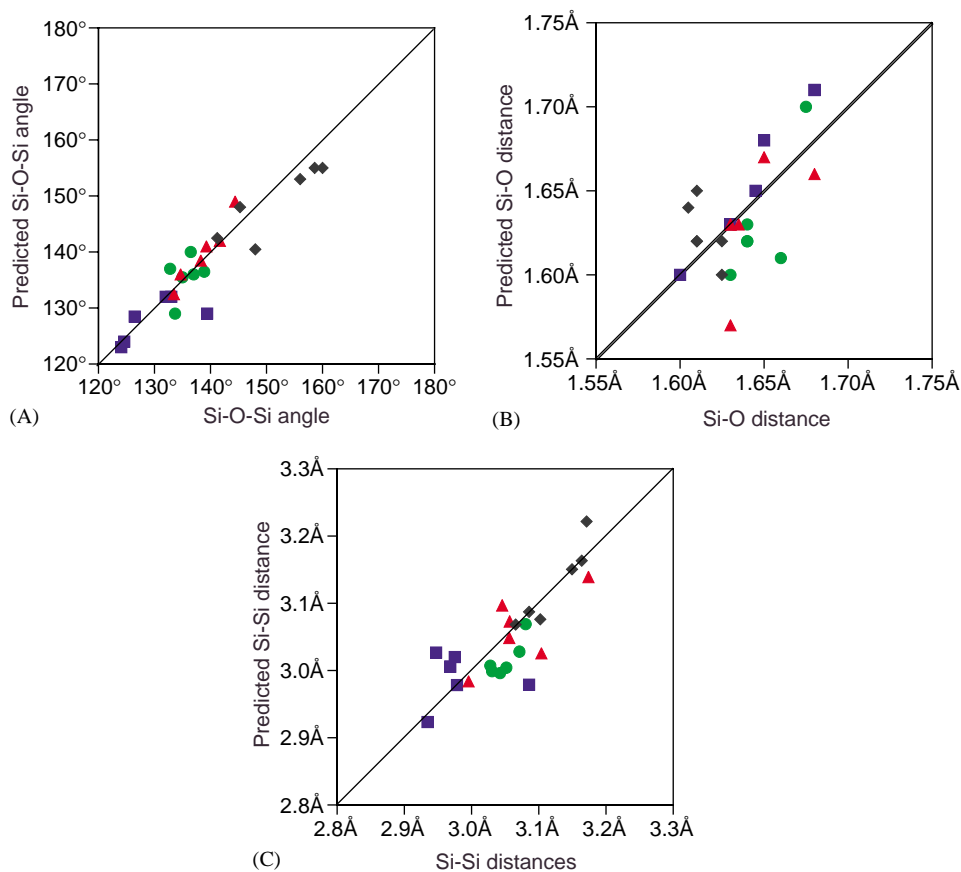


Fig. 6. Comparison between the predicted (A) Si–O–Si angle, (B) Si–O distance, and (C) Si–Si distance, which are based on the calculated  $^{17}\text{O}$  quadrupolar coupling parameters, with corresponding quantities reported from X-ray crystallography. Solid diagonal lines represent perfect agreement. Triangle (red) symbols are potassium modified sites, Circle (green) symbols are sodium modified, square (blue) symbols are lithium modified, and diamond (black) symbols do not have modifier cations.

oxygen atom in order to choose the correct expression for Eq. (1). Clearly, an assumption of this kind is most important for the lithium silicates because the shift in  $C_q$  due to the presence of Li-cations is greatest for this cation among the alkalis. The predicted Si–O distances using this approach are in good agreement with the actual distances, with the majority being within  $0.02 \text{ \AA}$  of the predicted value. It is noteworthy that, as was the case for silica polymorphs, the simultaneous measurement of  $C_q$  and  $\eta_q$  for each bridging oxygen site can be used to obtain the correlation between Si–O–Si angle and Si–O distance.

In summary, general trends in the  $^{17}\text{O}$  quadrupolar coupling parameters for bridging oxygen atoms in alkali silicates have been described based on ab initio self-consistent field Hartree–Fock molecular orbital calculations on silicate clusters. These results were calibrated by performing band-structure calculations based on the density functional theory for a variety of crystalline alkali silicates. As suggested by earlier investigations, the quadrupolar asymmetry parameter was found to be dependent on the Si–O–Si angle and the nature of the

modifier cation. The quadrupolar coupling constant was found to have a strong dependence on Si–O distance, as well as Si–O–Si angle and the nature of the modifier cation. Having established the manner in which local structural parameters influence the  $^{17}\text{O}$  quadrupolar coupling parameters, it is now possible to gain significant insights into the structure of alkali silicate glasses. Perhaps most noteworthy, it should now be possible to investigate correlated structural distributions for alkali-modified glasses by NMR, a significant achievement that is not presently possible by other experimental techniques.

#### Acknowledgment

This material is based upon work supported by the National Science Foundation under Grants CHE 0111109 (PJG). Any opinions, findings and conclusions or recommendations expressed in this material are those of the author(s) and do not necessarily reflect the views of the National Science Foundation.

## References

- [1] P.L. Bryant, C.R. Harwell, K. Wu, F.R. Fronczek, R.W. Hall, L.G. Butler, Single-crystal Al-27 NMR of andalusite and calculated electric field gradients: the first complete NMR assignment for a 5-coordinate aluminum site, *J. Phys. Chem. A* 103 (1999) 5246–5252.
- [2] P. Blaha, K. Schwarz, P.H. Dederichs, 1st-principles calculation of the electric-field gradient in HCP metals, *Phys. Rev. B* 37 (6) (1988) 2792–2796.
- [3] P. Blaha, K. Schwarz, P. Herzig, 1st-principles calculation of the electric-field-gradient of Li<sub>3</sub>N, *Phys. Rev. Lett.* 54 (11) (1985) 1192–1195.
- [4] B. Winkler, P. Blaha, K. Schwarz, Ab initio calculation of electric-field gradient tensors of forsterite, *Am. Mineral.* 81 (1996) 545–549.
- [5] A.R. Organov, G.D. Price, J.P. Brodholt, Theoretical investigation of metastable Al<sub>2</sub>Si<sub>2</sub>O<sub>5</sub> polymorphs, *Acta Crystallogr. B* 27 (1971) 2133–2139.
- [6] D.W. Mitchell, T.P. Das, W. Potzel, W. Schiessl, H. Karzel, M. Steiner, M. Kofferlein, U. Hiller, G.M. Kalvius, A. Martin, W. Schafer, G. Will, I. Halevy, J. Gal, Ab initio electric-field gradients and electron densities at Al-27, Fe-57, and Zn-67 in the spinels ZnAl<sub>2</sub>O<sub>4</sub> and ZnFe<sub>2</sub>O<sub>4</sub>, *Phys. Rev. B* 53 (1996) 7684–7698.
- [7] A.S. Brown, M.A. Spackman, Ab initio cluster calculations of the electron-density and electric-field gradient in corundum, *J. Phys. Chem. A* 96 (1992) 9200–9204.
- [8] S. Nagel, Cluster calculation of electronic-structure and quadrupole interaction in alpha-Al<sub>2</sub>O<sub>3</sub>, *J. Phys. C: Solid State* 18 (19) (1985) 3673–3685.
- [9] S. Nagel, Cluster calculation of electronic-structure and hyperfine interactions for alpha-Fe<sub>2</sub>O<sub>3</sub>, *J. Phys. Chem. Solids* 46 (8) (1985) 905–919.
- [10] R. Dovesi, M. Causa, R. Orlando, C. Roetti, V.R. Saunders, Ab initio approach to molecular crystals—a periodic Hartree–Fock study of crystalline urea, *J. Chem. Phys.* 92 (1990) 7402–7411.
- [11] M. Iglesias, K. Schwarz, P. Blaha, D. Baldomir, Electronic structure and electric field gradient calculations of Al<sub>2</sub>SiO<sub>5</sub> polymorphs, *Phys. Chem. Miner.* 28 (2001) 67–75.
- [12] M. Profeta, F. Mauri, C.J. Pickard, Accurate first principles prediction of O-17 NMR parameters in SiO<sub>2</sub>: assignment of the zeolite ferrierite spectrum, *J. Am. Chem. Soc.* 125 (2003) 541–548.
- [13] T. Charpentier, S. Ispas, M. Profeta, F. Mauri, C.J. Pickard, First-principles calculation of <sup>17</sup>O, <sup>29</sup>Si, and <sup>23</sup>Na NMR spectra of sodium silicate crystals and glasses, *J. Phys. Chem. B* 108 (2004) 4147–4161.
- [14] T.M. Clark, P.J. Grandinetti, Dependence of bridging oxygen <sup>17</sup>O quadrupolar coupling parameters on Si–O distance and Si–O–Si angle, *J. Phys.: Condens. Matter* 15 (2003) S2387–2395.
- [15] T.M. Clark, P.J. Grandinetti, P. Florian, J.F. Stebbins, Correlated structural distributions in silica glass, *Phys. Rev. B* 70.
- [16] K.E. Vermillion, P. Florian, P.J. Grandinetti, Relationships between bridging oxygen <sup>17</sup>O quadrupolar coupling parameters and structure in alkali silicates, *J. Chem. Phys.* 108 (17) (1998) 7274–7285.
- [17] T.M. Clark, P.J. Grandinetti, P. Florian, J.F. Stebbins, An <sup>17</sup>O NMR investigation of crystalline sodium metasilicate: implications for the determination of local structure in alkali silicates, *J. Phys. Chem. B* 105 (2001) 12257–12265.
- [18] T.M. Clark, P.J. Grandinetti, Relationships between bridging oxygen <sup>17</sup>O quadrupolar coupling parameters and structure in germanates, *J. Non-Cryst. Solids* 265 (2000) 75–82.
- [19] T.M. Clark, P.J. Grandinetti, Factors influencing the <sup>17</sup>O quadrupole coupling constant in bridging oxygen environments, *Solid State NMR* 16 (2000) 55–62.
- [20] J.A. Tossell, P. Lazzeretti, Calculation of NMR parameters for bridging oxygens in H<sub>3</sub>T-O-T'H<sub>3</sub> linkages (T, T' = Al, Si, P), for oxygen in SiH<sub>3</sub>O<sup>-</sup>, SiH<sub>3</sub>OH and SiH<sub>3</sub>OMg<sup>+</sup> and for bridging fluorine in H<sub>3</sub>SiF<sub>3</sub>SiH<sub>3</sub><sup>+</sup>, *Phys. Chem. Miner.* 15 (1988) 564.
- [21] C.G. Lindsay, J.A. Tossell, Ab Initio calculations of <sup>17</sup>O and <sup>27</sup>Al NMR parameters (<sup>27</sup>Al = <sup>31</sup>P, <sup>29</sup>Si) in H<sub>3</sub>TOTH<sub>3</sub> dimers and T<sub>3</sub>O<sub>9</sub> trimeric rings, *Phys. Chem. Miner.* 18 (1991) 191.
- [22] J.A. Tossell, P. Lazzeretti, Ab Initio calculations of oxygen nuclear quadrupolar coupling constants and oxygen and silicon NMR shielding constants in molecules containing Si–O bonds, *Chem. Phys. Lett.* 112 (1987) 205.
- [23] M.J. Frisch, G.W. Trucks, H.B. Schlegel, G.E. Scuseria, M.A. Robb, J.R. Cheeseman, V.G. Zakrzewski, J.J.A. Montgomery, R.E. Stratmann, J.C. Burant, S. Dapprich, J.M. Millam, A.D. Daniels, K.N. Kudin, M.C. Strain, O. Farkas, J. Tomasi, V. Barone, M. Cossi, R. Cammi, B. Mennucci, C. Pomelli, C. Adamo, S. Clifford, J. Ochterski, G.A. Peterson, P.V. Ayala, Q. Cui, K. Morokuma, D.K. Malick, A.D. Rabuck, K. Raghavachari, J.B. Foresman, J. Cioslowski, J.V. Ortiz, B.B. Stefanov, G. Liu, A. Liashenko, P. Piskorz, I. Komaromi, R. Gomperts, R.L. Martin, D.J. Fox, T. Keith, M.A. Al-Laham, C.Y. Peng, A. Nanayakkara, C. Gonzalez, M. Challacombe, P.M.W. Gill, B. Johnson, W. Chen, M.W. Wong, J.L. Andres, C. Gonzalez, M. Head-Gordon, E.S. Replogle, J.A. Pople, Gaussian 98, revision a.6, Gaussian, Inc. Pittsburgh, PA, 1998.
- [24] J.P. Perdew, K. Burke, M. Ernzerhof, Generalized gradient approximation made simple, *Phys. Rev. Lett.* 77 (18) (1996) 3865–3868.
- [25] D.J. Singh, Plane Waves, Pseudopotentials and the LAPW Method, Kluwer Academics, Boston, 1994.
- [26] P. Blaha, K. Schwarz, J. Luitz, WIEN97, a full potential linearized augmented plane wave package for calculating crystal properties, Karlheinz Schwarz, Technical University Wien, Austria, 1999.
- [27] H. Voellenkle, Verfeinerung der kristallstrukturen von Li<sub>2</sub>SiO<sub>3</sub> und Li<sub>2</sub>GeO<sub>3</sub>, *Z. Kristallogr.* 154 (1981) 77–81.
- [28] H. Seeman, Die kristallstruktur des lithiummetasilikates (Li<sub>2</sub>SiO<sub>3</sub>)<sub>x</sub>, *Acta Crystallogr.* 9 (1955) 251–252.
- [29] B.A. Maksimov, Y. Kharitonov, V.V. Ilyukhin, N.V. Belov, Crystal structure of lithium metasilicate, Li<sub>2</sub>SiO<sub>3</sub>, *Doklady Akad. Nauk. SSSR.*
- [30] K.F. Hesse, Refinement of the crystal structure of lithium polysilicate, *Acta Crystallogr. B* 33 (1977) 901–902.
- [31] R.I. Smith, R.A. Howe, A.R. West, A. Aragon-Pina, M.E. Villfuerte-Castrejon, The structure of metastable lithium disilicate Li<sub>2</sub>Si<sub>2</sub>O<sub>5</sub>, *Acta Crystallogr. C* 46 (1990) 363–365.
- [32] R.I. Smith, A.R. West, I. Abrahams, P.G. Bruce, Rietveld structure refinement of metastable lithium disilicate using synchrotron X-ray powder diffraction data from Daresbury SRS 8.3 diffractometer, *Powder Diffraction* 5 (1990) 137–143.
- [33] W.S. McDonald, D.J. Cruickshank, A reinvestigation of the structure of sodium metasilicate, Na<sub>2</sub>SiO<sub>3</sub>, *Acta Crystallogr.* 22 (1967) 37–43.
- [34] A.K. Pant, *Acta Crystallogr. B* 24 (1968) 1077–1083.
- [35] A.K. Pant, D.W. Cruickshank, The crystal structure of α-Na<sub>2</sub>Si<sub>2</sub>O<sub>5</sub>, *Acta Crystallogr. B* 24 (1968) 13–19.
- [36] M.E. Fleet, G.S. Henderson, Sodium trisilicate—a new high-pressure silicate structure (Na<sub>2</sub>Si[Si<sub>2</sub>O<sub>7</sub>]), *Phys. Chem. Miner.* 22 (1995) 383–386.
- [37] D.K. Swanson, C.T. Prewitt, The crystal structure of K<sub>2</sub>Si<sup>VI</sup>Si<sup>IV</sup>O<sub>9</sub>, *Am. Miner.* 68 (1983) 581–585.
- [38] H. Schweinsberg, F. Liebau, Die kristallstruktur des K<sub>4</sub>Si<sub>18</sub>O<sub>18</sub>: ein neuer silikat-schichttyp, *Acta Crystallogr. B* 24 (1982) 1968.
- [39] H. Maekawa, P. Florian, D. Massiot, H. Kiyono, M. Nakamura, Effect of alkali metal oxide on <sup>17</sup>O NMR parameters and Si–O–Si



- angles of alkali metal disilicate glasses, *J. Phys. Chem.* 100 (17) (1996) 5525–5532.
- [40] X. Xue, J.F. Stebbins, M. Kanzaki, Correlations between  $^{17}\text{O}$  NMR parameters and local structure around oxygen in high-pressure silicates: implications for the structure of silicate melts at high pressure, *Am. Miner.* 79 (1994) 31.
- [41] B. Zhou, Quantum calculations of quadrupolar interaction parameters for NMR spectroscopy and their significance for mineral structures, Ph.D. Thesis, University of Manitoba, 2003.
- [42] X. Xue, M. Kanzaki, Correlations between  $^{29}\text{Si}$ ,  $^{17}\text{O}$  and  $^1\text{H}$ , NMR properties and local structures in silicates: ab initio calculation, *Phys. Chem. Miner.* 26 (1998) 14–30.
- [43] X. Xue, M. Kanzaki, An ab initio calculation of  $^{17}\text{O}$  and  $^{29}\text{Si}$  NMR parameters for  $\text{SiO}_2$  polymorphs, *Solid State NMR* 16 (2000) 245–259.
- [44] X. Xue, M. Kanzaki, NMR characteristics of possible oxygen sites in aluminosilicate glasses and melts: an ab initio study, *J. Phys. Chem. B* 103 (1999) 10816–10830.